European Journal of Pharmacology 907 (2021) 174244

Contents lists available at ScienceDirect

European Journal of Pharmacology

journal homepage: www.elsevier.com/locate/ejphar

Full length article

# Synthesis, molecular docking, dynamic simulation and pharmacological characterization of potent multifunctional agent (dual GPR40-PPARγ agonist) for the treatment of experimental type 2 diabetes

Sergio Hidalgo-Figueroa [a,*], Ana Rodríguez-Luévano [b,1], Julio C. Almanza-Pérez [c], Abraham Giacoman-Martínez [d], Rolffy Ortiz-Andrade [e], Ismael León-Rivera [f], Gabriel Navarrete-Vázquez [g]

[a] CONACyT, IPICYT/Consorcio de Investigación, Innovación y Desarrollo para Las Zonas Áridas, San Luis Potosí, 78216, Mexico
[b] Posgrado en Biología Molecular, División de Biología Molecular, Instituto Potosino de Investigación Científica y Tecnológica (IPICYT), San Luis Potosí, 78216, Mexico
[c] Laboratorio de Farmacología, Depto. Ciencias de La Salud, D.C.B.S, Universidad Autónoma Metropolitana- Iztapalapa, Apdo.-Postal 55-535, México, CP 09340, CDMx, Mexico
[d] Departamento de Farmacobiología, Centro de Investigación y Estudios Avanzados Del Instituto Politécnico Nacional, Sede Sur, CDMx, Mexico
[e] Área de Farmacología Experimental, Laboratorio de Farmacología, Facultad de Química, Universidad Autónoma de Yucatán, Calle 43 No. 613 X Calle 90, Colonia Inalámbrica, Mérida, Yucatán, 97069, Mexico
[f] Centro de Investigaciones Químicas, IICBA, Universidad Autónoma Del Estado de Morelos, Cuernavaca, Morelos, 62209, Mexico
[g] Facultad de Farmacia, Universidad Autónoma Del Estado de Morelos, Cuernavaca, Morelos, 62209, Mexico

ARTICLE INFO

*Keywords:*
PPARγ
GPR40
Multifunctional
Antidiabetic
Molecular dynamics

ABSTRACT

The current manuscript describes two molecules that were designed against PPARγ and GPR40 receptors. The preparation of the compounds was carried out following a synthetic route of multiple steps. Then, the mRNA expression levels of *PPARγ*, *GLUT4,* and *GPR40* induced by compounds were measured and quantified in adipocyte and β-pancreatic cell cultures. The synthesized compound 1 caused an increase in the 4-fold expression of mRNA of *PPARγ* regarding the control and had a similar behavior to the pioglitazone, while compound 2 only increased 2-fold the expression. Also, the compound 1 increased to 7-fold the *GLUT4* expression levels, respect to the control and twice against the pioglitazone. On the other hand, the 1 increase 3-fold GPR40 expression, and compound 2 had a minor activity. Besides, 1 and 2 showed a moderated increase on insulin secretion and calcium mobilization versus the glibenclamide. Based on the molecular docking studies, the first compound had a similar conformation to co-crystal ligands into the binding site of both receptors. The poses were docked keeping the most important interactions and maintaining the interaction along the Molecular Dynamics simulation (20 ns). Finally, compound (1) showed an antihyperglycemic effect at 5 mg/kg, however at higher doses of 25 mg/kg it controlled blood glucose levels associated with feeding intake and without showing the adverse effects associated with insulin secretagogues (hypoglycemia). For these reasons, we have concluded that molecule 1 acts as a dual PPARγ and GPR40 agonist offering a better glycemic control than current treatments.

## 1. Introduction

Diabetes Mellitus (DM) is a chronic disease that has been characterized by hyperglycemia, with alterations in the metabolism of carbohydrates, lipids, and proteins (Baynest, 2015). According to the International Diabetes Federation (IDF), in 2019 there were 463 million people affected by diabetes in the world, and it has been estimated that in 2045 there will be 700 million (IDF, 2020). Type 2 Diabetes (T2D) is related to an insulin resistance, unbalanced secretion of insulin, pancreatic β-cell apoptosis, and an increased production of hepatic glucose (Vieira et al., 2019).

Unfortunately, the main factor in the development of diabetes is

* Corresponding author. CONACyT, Instituto Potosino de Investigación Científica y Tecnológica/ Consorcio de Investigación, Innovación y Desarrollo para las Zonas Áridas, Camino a la Presa San José 2055, Lomas 4a secc., San Luis Potosí, C.P. 78216, Mexico.
*E-mail address:* sergio.hidalgo@ipicyt.edu.mx (S. Hidalgo-Figueroa).
[1] Taken in part from the M. Experimental Biology thesis of A. Rodríguez-Luévano.

https://doi.org/10.1016/j.ejphar.2021.174244
Received 10 February 2021; Received in revised form 5 June 2021; Accepted 7 June 2021
Available online 8 June 2021
0014-2999/© 2021 Elsevier B.V. All rights reserved.

central obesity, especially visceral adipose tissue (Papaetis et al., 2015). Also, in adipocytes, there is a high expression of a peroxisome proliferator-activated receptor-γ (PPARγ); which is a transcription factor that when it is activated by a ligand, it regulates the carbohydrate metabolism and decreases the blood lipid levels (Gao et al., 2015; Hidalgo-Figueroa et al., 2017). Moreover, an augmented expression of PPARγ in adipose tissue leads to a reduction of insulin resistance by increasing the expression of the glucose transporter type 4 (GLUT4), which is responsible for the glucose uptake (Parimala et al., 2015).

Additionally, the G protein-coupled receptor 40 (GPR40) is a novel and attractive pharmacological target which complements the treatment through the control of other factors that frequently affect the diabetic patient, for example insulin deficiency. The novel target stimulates the secretion of insulin through its natural ligands; the free fatty acids (FFA) having a high level of expression in pancreatic beta cells (Rodrigues et al., 2017). This mechanism has a low risk of hypoglycemia because GPR40 has its effects on the second phase of insulin secretion (Hidalgo-Figueroa et al., 2017; Liu et al., 2014). However, studies have been carried out to develop new hybrid molecules based on a phenoxyacetic acid substructure that has a balanced dual agonism in PPARγ and GPR40 receptors (Darwish et al., 2018; Hidalgo-Figueroa et al., 2017).

For these reasons, we decided to perform the synthesis, pharmacological evaluation, and *in silico* studies of two novel molecules with an antihyperglycemic action. In this study, two phenoxyacetic derivatives against two important therapeutic targets in the treatment of diabetes: PPARγ and GPR40 receptors were designed. Also, molecular docking studies to determine the conformation and occupation into the binding site of both receptors were performed.

## 2. Material and methods

### 2.1. Chemistry

Unaltered and unpurified commercially chemicals and solvents were used in the following investigation. First, the melting points (m.p.) were taken into an open glass capillary and uncorrected using the Stuart SMP10 digital melting point apparatus from Cole-Parmer. Then, their reactions were examined through a thin-layer chromatography (TLC) on 0.2 mm precoated Silica Gel 60 F254 plates (E. Merck). Next, the $^{1}H$ and $^{13}C$ NMR spectra were recorded with a Varian Inova 400 MHz (9.4 T), the chemical shifts were given in ppm relative to tetramethylsilane (TMS) in DMSO-$d_6$. High-Resolution mass spectra were obtained from an Agilent 6545 LC/Q-TOF. Finally, the GC-MS analysis was performed by using a Hewlett Packard 6890 A gas chromatograph coupled to a Hewlett Packard Mass Selective Detector MSD 5970.

#### 2.1.1. {4-[2-(4-acetamidophenoxy)acetamido]phenoxy}acetic acid (1)

A 10 ml solution of ethyl {4-[2-(4-acetamidophenoxy)acetamido] phenoxy}acetate (3, 0.2 g, 0.5 mmol) and KOH (0.058 g, 1.0 mmol) in $H_2O$/EtOH (1:3 ratio) was stirred and refluxed until the reaction was completed (2.5 h). Then, this mixture was poured into water and acidified with HCl (5%) at a pH value of 3; the resulting precipitate (white solid) was filtered in vacuum and purified by column chromatography (mixture of eluents: $CH_2Cl_2$–EtOH in 90:10 ratio). Eventually, the obtained product was dried to give 0.139 g of a white compound. Yield 74%, m. p. 248–250 °C. $^{1}H$ NMR (400 MHz, DMSO-$d_6$) δ: 2.0 (s, 3H, H-14), 4.29 (s, 2H, H-8), 4.70 (s, 2H, H-11), 6.79 (d, 2H, H-2, H-6, $J = 7$ Hz), 6.91 (d, 2H, H-2′, H-6′, $J = 7$ Hz), 7.47 (d, 2H, H-3, H-5, $J = 7$ Hz), 7.49 (d, 2H, H-3′, H-5′, $J = 7$ Hz), 9.85 (s, 1H, NH-12), 9.95 (s, 1H, NH-9). $^{13}C$ NMR (100 MHz, DMSO-$d_6$) δ: 23.81 (O═C–$CH_3$, C-14), 65.0 (O–$CH_2$–C═O, C-8), 66.85 (O–$CH_2$–C═O, C-11), 114.37 (=CH–CH = , C-2, C-6), 114.76 (=CH–CH = , C-2′, C-6′), 120.48 (=CH–CH = , C-3, C-5), 121.23 (=CH–CH = , C-3′, C-5′), 132.11 (=C–N, C-4), 133.17 (=C–N, C-4′), 153.58 (=C–O, C-1), 154.94 (=*C*–O, C-1’), 166.12 (*O* = *C*-($CH_3$) N–H, C-13), 167.85 (O═C–($CH_2$)N–H, C-10), 170.73 ($CH_2$–*C*OOH, C-7). HRMSESI 358.3446 (calculated 358.3448).

#### 2.1.2. {4-[2-(4-acetylphenoxy)acetamido]phenoxy}acetic acid (2)

A 10 ml solution of ethyl {4-[2-(4 acetylphenoxy)acetamido]phenoxy}acetate (4, 0.2 g, 0.5 mmol) and KOH (0.060 g, 1.0 mmol) in $H_2O$/EtOH (1:3 ratio). The solution was stirred and refluxed until the reaction was completed (2.5 h). Then, this mixture was poured into water and acidified with HCl (5%) at pH value of 3; the resulting precipitate (white solid) was filtered in vacuum and purified using column chromatography (mixture of eluents: $CH_2Cl_2$–EtOH in 90:10 ratios). Next, the obtained product was dried to give 0.106 g of a white compound. Yield 57%, m. p. 210–212 °C. $^{1}H$ NMR (400 MHz, DMSO-$d_6$) δ: 2.5 (s, 3H, O═C–$CH_3$, H-13), 4.62 (s, 2H, O–$CH_2$–C═O, H-8), 4.77 (s, 2H, O–$CH_2$ − C═O, H-11), 6.87 (d, 2H, =CH–CH = , H-2, H-6, $J = 9.08$ Hz), 7.08 (d, 2H, =CH–CH = , H-2′, H-6′, $J = 8.94$ Hz), 7.51 (d, 2H, =CH–CH = , H-3, H-5, $J = 9.07$ Hz), 7.93 (d, 2H, =CH–CH = , H-3′, H-5′, $J = 9.01$ Hz), 10.0 (s, 1H, O═C–N–H, NH-9). $^{13}C$ NMR (100 MHz, DMSO-$d_6$) δ: 26.52 (O═C–$CH_3$, C-13), 64.7 (O–CH 2 –C═O, C-8), 67.1 (O–$CH_2$ − C═O, C-11), 114.6 (=CH–CH = , C-2, C-6), 114.6 (=CH–CH = , C-2′, C-6′), 121.3 (=CH–CH = , C-3, C-5), 130.2 (=C–C═O, C-4′) 130.5 (=CH–CH = , C-3′, C-5′), 131.8 (=C–N, C-4), 154.1 (=C–O, C-1), 161.7 (=C–O, C-1’), 165.6 (O═C–OH, C-7), 170.3 (O═C–N–H, C-10), 196.4 ($CH_3$ − *C* = *O*, C-12). HRMSESI 343.3281 (calculated 343.3284).

#### 2.1.3. Ethyl {4-[2-(4-acetamidophenoxy)acetamido]phenoxy}acetate (3)

A 30 ml solution of *N*-(4-hydroxyphenyl)acetamide (0.1685 g, 1.1 mmol) and $K_2CO_3$ (0.2289 g, 1.6 mmol) was stirred in acetonitrile at room temperature (27 °C) for 30 min. Immediately, the compound 5 (ethyl [4-(2-chloroacetamido)phenoxy]acetate, 0.3 g, 0.0001 mol) was slowly added. The reaction was monitored by thin-layer chromatography until the reagents were consumed (17 h). Once the reaction was completed, the mixture was poured into cold water and it was stirred during 20 min, and the resulting precipitate was filtered. Finally, the product that was obtained was dried to give 0.309 g of a white compound. Yield 72%, m. p. 163–165 °C. $^{1}H$ NMR (400 MHz, DMSO-$d_6$) δ: 1.2 (t, 3H, H-16, $J = 8$ Hz), 2.0 (s, 3H, H-14), 4.16 (q, 2H, H-15, $J = 8$ Hz), 4.60 (s, 2H, H-11), 4.70 (s, 2H, H-8), 6.89 (d, 2H, H-2, H-6, $J = 5$ Hz), 6.93 (d, 2H, H-2′, H-6′, $J = 5$ Hz), 7.49 (d, 2H, H-3, H-5, $J = 5$ Hz, 7.55 (d, 2H, H-3′, H-5′, $J = 5$ Hz), 9.88 (s, 1H, H-12), 9.95 (s, 1H, H-9). $^{13}C$ NMR (100 MHz, DMSO-$d_6$) δ: 14.05 (–$CH_2$–$CH_3$, C-16), 23.81 (O═C–CH, C-14), 60.6 ($CH_3$–$CH_2$–O, C-15), 65.0 (O–$CH_2$–C═O, C-8), 67.50 (O–$CH_2$–C═O, C-11), 114.37 (=CH–CH = , C-2, C-6), 114.76 (=CH–CH = , C-2′, C-6′), 120.6 (=CH–CH = , C-3, C-5), 121.3 (=CH–CH = , C-3′, C-5′), 132.17 (=C–N, C-4), 133.27 (=C–N, C-4′), 153.58 (=C–O, C-1), 153.94 (=C–O, C-1’), 166.12 (O═C–($CH_3$)N–H, C-10), 167.85 (O═C–($CH_2$)N–H, C-13), 170.73 (O═C–O–$CH_2$, C-7). HRMSESI 384.3829 (calculated 384.3830).

#### 2.1.4. Ethyl {4-[2-(4-acetylphenoxy)acetamido]phenoxy}acetate (4)

A 30 ml solution of 1-(4-hydroxyphenyl)ethan-1-one (0.1518 g, 1.1 mmol) and $K_2CO_3$ (0.2288 g, 1.6 mmol) in acetonitrile. The previous mixture was stirred at room temperature (27 °C) for 30 min. Immediately, a compound 5 (ethyl [4-(2-chloroacetamido)phenoxy]acetate, 0.3 g, 0.0001 mol) was slowly added. The reaction was monitored with the thin-layer chromatography until the reagents were consumed (17 h). Once the reaction was completed, the mixture was poured into cold water and stirred for 20 min, the resulting precipitate was filtered. Finally, the obtained product was dried to give 0.305 g of a white compound. Yield 74%, m. p. Of 115–117 °C. $^{1}H$ NMR (400 MHz, DMSO-$d_6$) δ: 1.21 (t, 3H, O–$CH_2$–$CH_3$, H-15, $J = 8$ Hz), 2.51 (s, 3H, O═C–$CH_3$, H-13), 4.16 (q, 2H, O–$CH_2$–$CH_3$, H-14, $J = 8$ Hz), 4.73 (s, 2H, O–$CH_2$–C═O, H-11), 4.78 (s, 2H, O–$CH_2$–C═O, H-8), 6.90 (d, 2H, =CH–CH = , H-2, H-6, $J = 9.08$ Hz), 7.10 (d, 2H, =CH–CH = , H-2′, H-6′, $J = 8.94$ Hz), 7.52 (d, 2H, =CH–CH = , H-3, H-5, $J = 9.07$ Hz), 7.95 (d, 2H, =CH–CH = , H-3′, H-5′, $J = 9.01$ Hz), 10.1 (s, 1H, O═C–N–H, H-9).$^{13}C$ NMR (100 MHz, DMSO-$d_6$) δ: 14.30 (O–$CH_2$–$CH_3$, C-15), 26.75 (O═C–$CH_3$, C-13), 60.9 (O–$CH_2$–$CH_3$, C-14), 65.1 (O–$CH_2$–C═O, C-8), 67.3 (O–$CH_2$–C═O, C-11), 114.9 (=CH–CH = , C-2, C-6), 115.1

(=CH–CH = , C-2′,C-6′), 121.6 (=CH–CH = , C-3, C-5), 130.7 (=CH–CH = , C-3′, C-5′), 131.8 (=C–N, C-4), 154.1 (=C–O, C-1), 161.5 (=C–O, C-1'), 166.2 (O=C–O–H, C-7), 169.3 (O=C–N–H, C-10), 196.2 ($CH_3$–C=O, C-12). HRMSESI 371.7051 (calculated 371.7054).

#### 2.1.5. Ethyl [4-(2-chloroacetamido)phenoxy]acetate (5)

The aniline 6 of the previous reactions (2.5 g, 12.8 mmol) and 2.67 ml of $Et_3N$ (19.2 mmol) were dissolved in $CH_2Cl_2$ (15 ml). The mixture was cooled down with an ice bath and 2-chloroacetyl chloride (1.02 ml, 12.9 mmol) were added dropwise to the cooled mixture. After, the ice bath was removed and the mixture was stirred at room temperature for 12 h. Then, the solvent was removed under a reduced pressure and cold water (30 ml) was added and the mixture was stirred during another 20 min. The resulting white precipitate was filtered, washed with cold water (3 × 10 ml) and dried. Yield 2.65 g (76%). m. p. 99.3–100.4 °C, $C_{12}H_{14}ClNO_4$ (271.7). Mass (EI) m/z (% rel. Int.) 271 (80, M+), 198 (20), 184 (30), 168 (10), 91 (10), 77 (159). Anal. Calc. $C1_2H_{14}ClNO_4$: C, 53.05; H, 5.19; N, 5.16. Found: C, 52.90; H, 5.14; N, 5.26.$^1$H RMN (500 MHz, $CDCl_3$) δ: 1.29 (t, 3H, $OCH_2CH_3$), 4.16 (s, 2H, H-2″), 4.26 (c, 2H, $OCH_2CH_3$), 4.60 (s, 2H, H-2), 6.88 (d, 2H, H-2′, H-6′, $J$ = 9.05 Hz), 7.45 (d, 2H, H-3′, H-5′, $J$ = 8.95 Hz), 8.29 (s, 1H, NH). $^{13}$C RMN (125 MHz, $CDCl_3$) δ: 14.16 ($OCH_2CH_3$), 42.85 (C-2″), 61.45 ($OCH_2CH_3$), 65.66 (C-2), 115.13 (C-2′, C-6′), 121.95 (C-3′, C-5′), 130.75 (C-4′), 155.14 (C-1′), 163.80 (C-1″), 168.83 (C-1).

#### 2.1.6. Ethyl (4-aminophenoxy)acetate (6)

A suspension of 2.5 g (11.1 mmol) of ethyl (4-nitrophenoxy)acetate (7) and 0.125 g of Pd/C 10% in 200 ml of ethanol was reduced with hydrogen at 4 lb/in$^2$ in a Parr hydrogenation reactor (500 ml). After 10 min, the reaction consumed 32 lb/in$^2$. Then, the catalyst was removed through careful filtration and the filtrate was concentrated under reduced pressure until there was a presence of a yellow liquid. This liquid was not purified and it was immediately used for the subsequent acylation reaction.

#### 2.1.7. Ethyl (4-nitrophenoxy)acetate (7)

A 30 ml solution of 4-nitrophenol 8 (1 g, 0.0072 mol) and $K_2CO_3$ (1.49 g, 0.0108 mol) in acetone. First, the mixture was stirred for 30 min. Then, 0.83 ml of ethyl bromoacetate 9 (0.0075 mol) was added on dropwise. The mixture was refluxed and monitored with a thin-layer chromatography until the raw material was converted (2.5 h). Consequently, the solvent was removed under reduced pressure. Later, cold water (10 ml) was added and the mixture was stirred for 30 min and the resulting precipitate was filtered, washed with cold water (3 × 15 ml) and recrystallized from ethanol obtaining a solid pale yellow. Yield 1.42 g (88%). m. p of 71.5–72.6 °C. $C_{10}H_{11}NO_5$ (225.2). Mass (EI) *m/z* (% int. Rel.) 225 (100, $M^+$), 152 (90), 122 (25). Anal. Calc. $C_{10}H_{11}NO_5$: C, 53.33; H, 4.92; N, 6.22. Found: C, 52.48; H, 4.89; N, 6.49.$^1$H RMN (500 MHz, $CDCl_3$) δ: 1.3 (t, 3H, $OCH_2CH_3$), 4.29 (c, 2H, $OCH_2CH_3$), 4.72 (s, 2H, H-2), 6.97 (dd, 2H, H-2′, H-6′, $J$ = 7.1 Hz), 8.21 (d, 2H, H-3′, H-5′, $J$ = 6.8 Hz). $^{13}$C RMN (125 MHz, $CDCl_3$) δ: 14.14 ($OCH_2CH_3$), 61.82 ($OCH_2CH_3$), 65.45 (C-2), 114.72 (C-2′, C-6′), 125.93 (C-3′, C-5'), 162.66 (C-1).

#### 2.1.8. N-(4-hydroxyphenyl)acetamide (acetaminophen)

The Acetaminophen was obtained from 10 commercial tablets (500 mg paracetamol, Lab Perrigo. GI) with a 17G102 lot number and expiration date of June 2019, they were powdered in a grinder and the resulting powder was dissolved in 20 ml of ethanol (99.5% v/v) for 5 min at room temperature. Subsequently, it was filtered under vacuum, and the solvent was eliminated until a white crystalline solid was obtained (4.7 g, 94%). Acetaminophen was checked by thin-layer chromatography and the melting point was measured 169–172 °C (reported m. p. 169–170 °C).

### 2.2. In vitro assay

#### 2.2.1. MTT assay

MTT [3-(4,5-dimethylthiazole-2-yl)-2,5-diphenyltetrazolium bromide] assay (NR, Sigma-Aldrich, MO, USA) was used to evaluate the cellular viability and cytotoxicity (Loveland et al., 1992) of compounds 1–4. Fibroblasts and RINm5F cells were grown in microplates that had 96 plates ($5 \times 10^3$ cells per well) in Dulbecco's modified Eagle's medium (DMEM medium) and Roswell Park Memorial Institute medium (RPMI 1640 medium), respectively. Exponential concentrations of title compounds were utilized and preincubated (0.5, 5, 50 and 100 μM) for 24 h (n = 4), which were measured at 570 nm (Loveland et al., 1992).

#### 2.2.2. 3T3-L1 line cell culture

The 3T3-L1 cells were cultured in 6-well plates at a semi-confluent density (45,000 cells/well) in Dulbecco's modified Eagle's medium supplemented with 25 mM glucose, 10% fetal bovine serum, 1 mM sodium pyruvate, 2 mM glutamine, 0.1 mM non-essential amino acids, and 1% (1000 U/ml) gentamicin, in a 5% $CO_2$ humidified atmosphere at 37 °C. After two days of confluence, the cell differentiation was carried out with 0.5 mM 3-isobutyl-1-methylxanthine, 0.25 mM dexamethasone acetate, and 80 mM bovine insulin, during 48 h, followed by insulin alone for another 48 h. The culture medium without insulin was changed every 2 days during 8 days of differentiation (Garcia-Macedo et al., 2008; Hidalgo-Figueroa et al., 2017).

#### 2.2.3. RINm5F line cell culture

RINm5F cells were seeded at a density of 80,000 cells/well in 6-well plates and were maintained in RPMI 1640 supplemented with 100 U/ml gentamicin, 10% FBS (v/v) (HyClone Laboratories, Logan, UT), 2 mM L-glutamine and 1 mM sodium pyruvate at 37 C and 5% $CO_2$, and 95% of humidity (Hidalgo-Figueroa et al., 2017; Jhun et al., 2013; Wu et al., 2015).

#### 2.2.4. PPARγ and GRP40 mRNA expression, measurement of $[Ca^{2+}]_i$ and measuring the insulin secretion

The objective of this work was to evaluate novel compounds with the previously published methodologies, without protocol modifications, equipment, or reagents (Hidalgo-Figueroa et al., 2017), but unlike preceding molecules, the compounds described in this manuscript were pre-incubated at 1 μM.

### 2.3. Antihyperglycemic in vivo assay in normoglycemic rats

#### 2.3.1. Animals

Normoglycemic male Wistar rats (6 weeks old, 150–200 g, body weight) were provided by the Animal house of Universidad Juárez Autónoma de Tabasco (UJAT). These animals were maintained at standard laboratory conditions; temperature (25 ± 2 °C), relative humidity 40–60%, 12 h light/dark cycle, having free access to food and tap water. The animals were allowed to acclimatize for two weeks before the experiments started. The experimental protocol was approved by the Institutional Animals Ethics Committee (3/2017) of Universidad Juárez Autónoma de Tabasco, and the animal care was taken as per the Guidelines of Mexican Official Norms for Animal Experimentation (NOM-062-ZOO-1999).

#### 2.3.2. Experimental design

The animals were divided into four groups. 1) The Control rats (group 1) were given 5 ml/kg of distilled water; 2) The Positive control (group 2) were given 5 mg/kg of glibenclamide (insulin secretagogue drug); 3) The treatment rats (group 3 and 4) were given 5 and 25 mg/kg of 1, respectively. The oral glucose tolerance test (OGTT) was performed in overnight fasted (16 h) for intragastric administration. The rat's groups (n = 5) time 0 h was set before any treatments; 30 min later, a dextrose dose (2 g/kg) was administered, and the blood samples were

obtained 0, 0.5, 1, 2, and 4 h post carbohydrate ingestion. Plasmatic glucose levels were measured with a commercial glucometer and glucose test strips (Accucheck Active, Roche) (Ortiz-Andrade et al., 2012).

### 2.4. Antihyperglycemic in vivo assay in diabetic rats

#### 2.4.1. Experimental diabetes induction

Experimental Type 2 Diabetes (T2D) was induced in overnight fasted animals by two intravenous injections of alloxan (Sigma-Aldrich) at intervals of 48 h (125 mg/kg). Diabetes was confirmed by the elevated blood glucose levels determined at 72 h and on the 7th day after the treatment (glucose level above 200 mg/dL was taken into account). Only the rats that were confirmed with T2D were used in the study (Calzada et al., 2017).

### 2.5. In silico

#### 2.5.1. GPR40 model preparation

The crystal structure of GPR40 (PDB access code: 5TZR, resolution of 2.2 Å) was prepared using the DockPrep in Chimera 1.14rc (Pettersen et al., 2004). First, the extra molecules such as ligands, solvent, non-complexed ions, or additional subunits were deleted. Then, the incomplete side chains of the structure were repaired using a set of the Dunbrack 2010 rotamer library (Shapovalov and Dunbrack, 2011) and all hydrogens and charges were added. After that, the molecule was saved in a PDB format using it in molecular docking and molecular dynamics simulations.

#### 2.5.2. Molecular docking studies

Molecular docking studies in compound 1 were carried out with PPARγ (2F4B) and GPR40 (5TZR, modified) crystal structures, and the docking calculations were conducted with the AutoDock Vina (Humphrey et al., 1996). All of the water molecules and also EHA (co-crystallographic ligand from PPARγ) and MK6 (co-crystallographic ligand from GPR40) were removed from the crystallographic structure. Then, each one of the hydrogen atoms were added, non-polar hydrogen atoms were merged and Gasteiger charges were assigned to the all molecules (ligands and proteins). Next, the torsions from compounds were allowed to rotate during the docking study. Each grid was centered at the crystallographic coordinates of EHA (center_x = 8.693; center_y = −6.961 and center_z = 39.672) and MK6 (center_x = −32.741; center_y = −3.538 and center_z = 58.465 of PPARγ and GPR40, respectively. The grid dimensions were 40 × 40 x 40 points and 58 × 40 x 40 points with a default spacing of PPARγ and GPR40, respectively. Finally, the exhaustiveness employed was 64.

#### 2.5.3. Molecular docking validation

The molecular docking protocol was validated through a re-docking of co-crystal ligands (EHA or MK6) into the binding site of both pharmacological targets. The conditions to reproduce the binding mode of co-crystallographic ligands were established and after a re-docking, we found that the root mean squares deviations (RMSD) between the co-crystal ligand and the re-docked structure were 0.53 Å to PPARγ and 1.6 Å to GPR40, which indicated that the parameters in docking simulations were worthy in reproducing orientation, conformation, and interactions in the original X-ray crystal structure. These conditions allowed us to obtain good predictions in the compounds of interest.

#### 2.5.4. Molecular dynamics simulations

Molecular dynamics (MD) were performed using the NAnoscale Molecular Dynamics (NAMD) software package (Phillips et al., 2005) and as a force field, the standard CHAMM-36 was used. The obtained complexes of compound 1 with PPARγ and GPR40 were used to perform the MD simulations. First, the obtained pose of compound 1 to each receptor was protonated and submitted to the LigParGen web-based server (http://zarbi.chem.yale.edu/ligpargen/) (Dodda et al., 2017a, 2017b; Jorgensen and Tirado-Rives, 2005). Second, the provided force field (FF) parameters in ligand (file.prm), the topology (file.rtf), and molecule structures (file.pdb) were retrieved and the files were used as input formats of recognition to NAMD. After, each protein-ligand complex was put into a cubic box, Just the GPR40 receptor or complexes (lig-GPR40) were embedded in the hydrated POPC (1-palmitoyl-2-oleoyl-sn-glycero-3-phosphocholine) membrane, which were used to simulate a lipid bilayer environment around the receptor (dimensions 71 × 69). In addition, the systems were solvated using the water model of TIP3P and neutralized by adding $Cl^-$ ions.

Then, the energy of these systems was immediately minimized from 2ps to 273.15 K with backbone restraints, followed by a heating protocol with 288 ps (this protocol was used only with the GPR40 complexed with bilayer lipid) and/or followed by an equilibration protocol with 100 ps of simulations at 300 K with backbone restraints. Next, 20 ns of MD simulation were performed at 300 K temperature, with the isothermal-isobaric (NpT) ensemble and periodic boundary conditions at a constant pressure of 1 atm without any restraints. During each one of the MD simulations, the Particle Mesh Ewald (PME) method was used with updates every 2 fs., consequently the MD simulations were prepared using QwikMD (Ribeiro et al., 2016).

Finally, the calculations were conducted using a workstation DELL Precision 7920 equipped with two Xeon® Gold® 5122 @ 3.60 GHz processor (Intel, US), 128 Gb of DDR memory and Quadro P4000 (NVIDIA, US) in our institute. Other software packages such as the Visual Molecular Dynamics (VMD) was employed as an interface, analyzer, and visualizer (Humphrey et al., 1996).

## 3. Results

### 3.1. Chemistry

The two phenoxyacetic acid derivatives (1 and 2) were synthesized through a series of linear transformations, the first reaction was started from compounds 8 and 9 to give the intermediate ether (7), which was subjected to the catalytic reduction with $H_2$ and Pd/C to obtain the aniline product (6) with a totally raw material conversion. Immediately, an acylation of ethyl (4-aminophenoxy)acetate (6) was carried out with 2-choroacetyl chloride giving the corresponding compound 5 in good yield. The intermediate 5 has been the most important common moiety used to synthesize the ester derivative compounds 3 and 4, from phenol reagents: *N*-(4-hydroxyphenyl)acetamide (acetaminophen) and 1-(4-hydroxyphenyl)ethan-1-one, respectively. Then, the Acetaminophen was isolated from commercial tablets with ethanol. Consequently, the compound 5 was subjected to $SN_2$ conditions with both phenol moieties to obtain the required ester intermediates 3 (ethyl {4-[2-(4-acetamidophenoxy)acetamido]phenoxy}acetate) and 4 (ethyl {4-[2-(4-acetylphenoxy) acetamido]phenoxy}acetate). Finally, the ester products were treated under basic conditions with KOH at reflux in EtOH-water to give the final compounds 1 and 2 in a moderate yield (Scheme 1).

Finally, all compounds and their intermediates were recovered with appropriate yields (±70%) and characterized by the $^1H$, $^{13}C$-Nuclear Magnetic Resonance and Mass Spectral Analysis. $^1H$-NMR spectra of compounds 1 and 2 showed classic aromatic signals that corresponded to a benzene system in the range of 6.79–8.21 ppm, the signals of the amide group were founded in a range of 9.85–10.0 ppm; the methylene was found at a range of 4.29–4.77 ppm, while the carboxylic group was assigned by $^{13}C$ spectra in which the signal was established at 165.6–170.7 ppm.

### 3.2. In vitro assays

#### 3.2.1. PPARγ, GPR40, GLUT-4 expression

Once compounds 1 and 2 have been evaluated with their respective prodrugs (esters: 3 and 4, respectively) in the MTT functionality test on

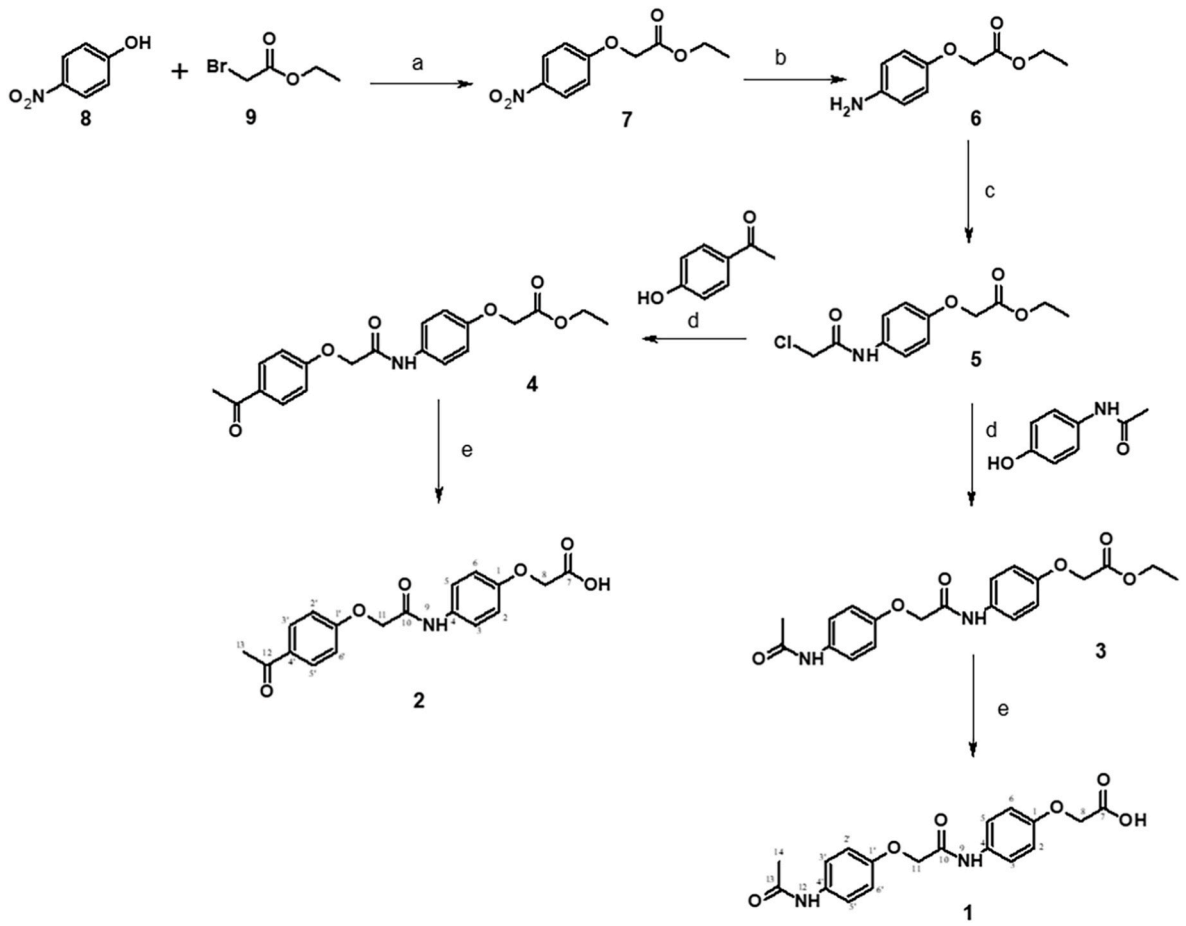


**Scheme 1.** Synthesis of phenoxyacetic acid derivatives, conditions and reagents: a) $K_2CO_3$, acetone, reflux; b) $H_2$ Pd/C 10% EtOH, r. t.; c) d) $K_2CO_3$, AcCN, reflux; e) KOH, EtOH–$H_2O$, reflux.

3T3-L1 and RINm5F culture cells. We found that in the range of 0.5 μM–50 μM, the molecules were safe to use and did not affect cell functionality (Fig. 1). Then, we decided to evaluate the effect in cell cultures of 3T3L1 and RINm5F at 1 μM to explore the overexpression of target genes.

Fig. 1 shows the results of tested compounds 1–4 in 3T3-L1 and RINm5F cells in different concentrations to determine and calculate the safety concentrations that do not affect the cellular functionality. The results shown in Fig. 2 support the objective of this research, since compound 1 shows a high PPARγ expression, almost 3 times the level of expression concerning to the control (CT) in adipocytes, but showing a similar effect as pioglitazone (3T3-L1 cell line, Fig. 2A). Nevertheless, the prodrugs of final compounds (3 and 4) did not show a relevant action on PPARγ expression, and compound 2 only presented an increase of 2-fold respect to CT, these results have been shown in Fig. 2A. However, the increment of PPARγ expression of compound 1 had an impact on GLUT4 expression levels, which are a very important target expressed PPARγ activation.

### 3.2.2. *Insulin secretion and [Ca2+]i in RINm5F cells*

In order to be able to corroborate that the increment on GPR40 expression led to an insulin release, we evaluated the 1 and 2 compounds in RINm5F cells, in which the insulin release as well as intracellular calcium release were involved in this event. Finally, a moderate secretion of insulin that supported our hypothesis, which meant that the designed compounds caused a low insulin release and did not cause hypoglycemia as glibenclamide (Fig. 2E) through the intracellular calcium quantification was observed.

### 3.3. *In vivo activity*

Compound 1 was evaluated in vivo using a rat model for non-insulin-dependent diabetes mellitus (NIDDM) and an additional group of normoglycemic rats with a complementary assay of oral glucose tolerance test (OGTT), respectively; glibenclamide was used as a positive control. The hypoglycemic and antihyperglycemic activity was determined using 5 or 25 mg/kg as a single dose, respectively.

As can be seen in Fig. 3A, compound 1 (dose of 5 mg/kg) did not induce hypoglycemia in normoglycemic rats compared to saline solution. However, compound 1 (5 mg/kg) decreased the hyperglycemic peak on the glucose tolerance test of the same normoglycemic animals, as well as glibenclamide (Fig. 3C). This indicates that compound 1 is able to control high blood glucose levels at basal levels but avoiding hypoglycemia. Afterwards, another OGTT was carried out in diabetic rats, for instance, rats that have high glucose values and also a dextrose intake; determining that compound 1 (dose of 5 mg/kg) also lowered the high glucose concentrations as glibenclamide, decreased to 50% at 7 h post-administration Fig. 3D). Nevertheless, when the compound was administered to the same diabetic model but with free feeding and tap water access, there was a loss effect observed at 5 mg/kg even if at a higher dose (25 mg/kg) the hyperglycemia were once again controlled once (Fig. 3B). This indicates that the lower dose is not effective because the feeding *ad libitum* increases the glucose level throughout the experiment, while a dose of 25 mg/kg accomplishes glucose control, even when there is a free feeding access (*ad libitum*).

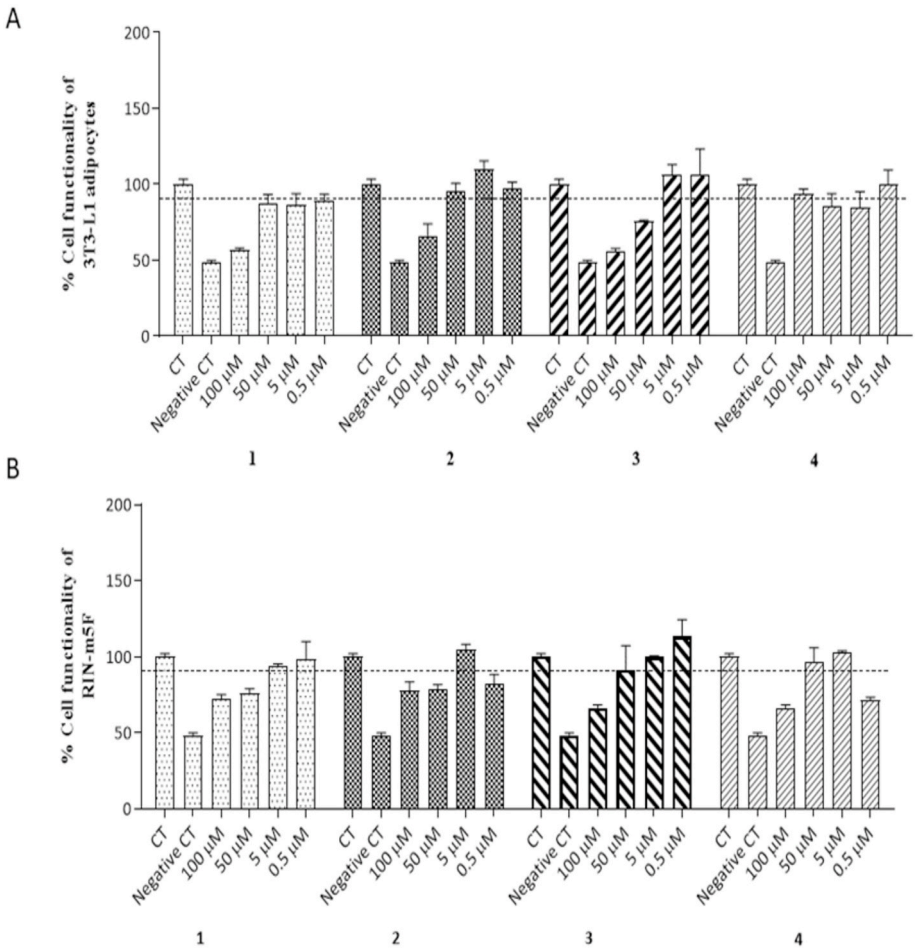


**Fig. 1.** Cell functionality test by reduction of MTT in 3T3-L1 cells and RIN-m5F. The compounds 1–4 are shown in different concentrations tested in 3T3-L1 (A) and RIN-m5F (B) cells.

### *3.4. Molecular docking of compound 1*

A molecular docking study to explain the outstanding activity showed by compound 1 on PPARγ and GPR40 structures, which was achieved to find the possible binding mode into the orthosteric site (active site) in both receptors was performed. Compound 1 was docked with a crystallographic structure of PPARγ (pdb code: 2f4b) and GPR40 (pdb code: 5tzr). This molecule showed a good affinity against both targets with free binding energy of −8.2 kcal/mol and −8.4 kcal/mol, respectively ($K_i = 0.7944 \pm 0.13$ μM). This can give us an indication that the affinity towards both receptors is similar, and could provide a dual equilibrate effect to this molecule. Fig. 4A–C shows the binding mode of 1 and co-crystal (MK6) into the GP40 receptor with a respective re-docking pose. We can observe in both figures, the conservation of three important interactions with Tyr90, Arg181, and Arg254 residues, where the first scaffold's portion of the ligands (1 and MK6) is centered between the transmembrane domains and the tail (acetaminophen and methylsulfonylpropoxy groups) are in the extra-domain. Therefore, in both cases, the acid region is primarily recognized and essential for binding to these therapeutic targets (Li et al., 2019a; Sum et al., 2007). The most recently published results by other research groups have demonstrated that FFA1 agonists bearing phenoxyacetic acid scaffold exerted a greater potential on glucose control than that of TAK-875 (Li et al., 2019b).

Regarding PPARγ, the results are shown in Fig. 4B–D, which illustrate the compound 1 and EHA into the binding site. We can observe in this representation that in both molecules had interactions at least with three residues of the binding site (His323, His449 and Tyr473), which are considered anchoring residues in this receptor since almost all of the ligands that activate this receptor are anchored to these amino acids. Moreover, we found a new interaction between Ser342 and the last C═O of the amidic group from compound 1.

### *3.5. Molecular dynamics simulation of most active compound (1) into PPARγ and GPR40*

The complexes obtained from molecular docking were used in the molecular dynamics simulation and it was performed to investigate the stability and possible variations of interactions between ligand and targets (GPR40 and PPARγ). The root mean squares deviations (RMSD) in complex with co-crystal compound, molecule 1, or in absence of ligands such as a number of H-bonds are illustrated in Figs. 5 and 6.

Regarding the complex of GPR40 during the progress of molecular dynamics simulation, the interactions were maintained with Tyr90, Arg181, and Arg254. However, a new interaction appeared between Leu 137 and nitrogen of the central amidic group of a molecule that increased the stability and the last overlaying of phenyl group with Phe 142 (Fig. 5A). This stability is correlated with RMSD obtained during MD (Fig. 5C), which was lower than 1.5 Å after 12 ns of simulation to compound 1, even lower than the co-crystallized ligand. Also, all the hydrogen bonds ranged between 3 and 4 during the entire simulation (Fig. 5B), impacting on the stability of the complex.

On the other hand, the protein in the absence of ligands shows a balanced variation in the RMSD throughout the simulation (Fig. 5C), but in the presence of the co-crystallized ligand, the protein structure is disturbed, while in the presence of compound 1, the protein structure

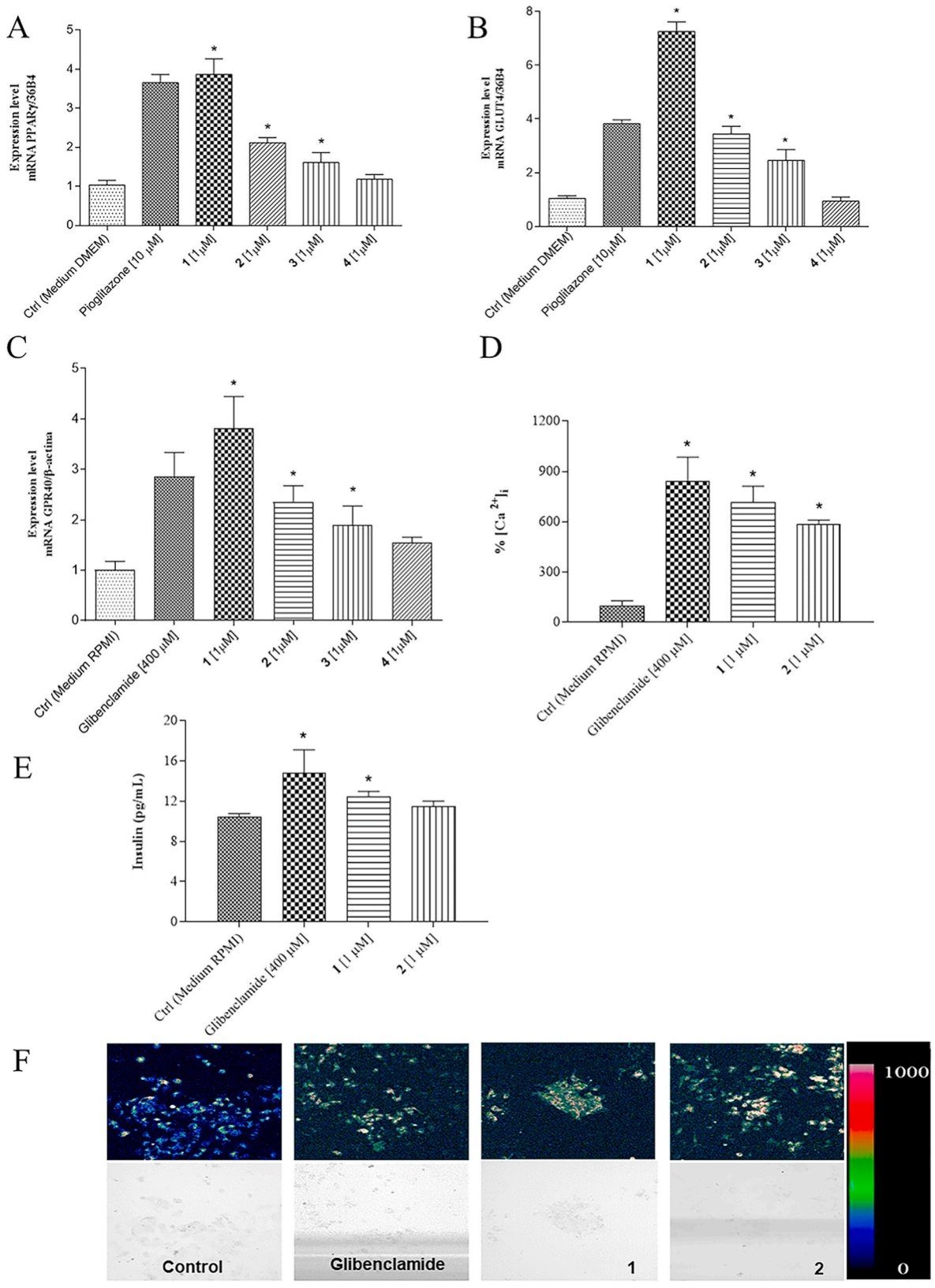


**Fig. 2.** Effect of compounds 1–4, pioglitazone and glibenclamide on mRNA expression levels of genes of interest: PPARγ (A), GLUT4 (B), GPR40 (C), Percentage of intracellular $Ca^{2+}$ concentration (D), insulin release (E) and Images confocal microscopy (Fluo-4 AM) of treated cells. Scale bar indicates the increase in $[Ca^{2+}]$ intracellular concentration (F). Results are expressed as relative expression of mRNA (mean ± S.E.M, n = 4) *p < 0.05 compared with control.

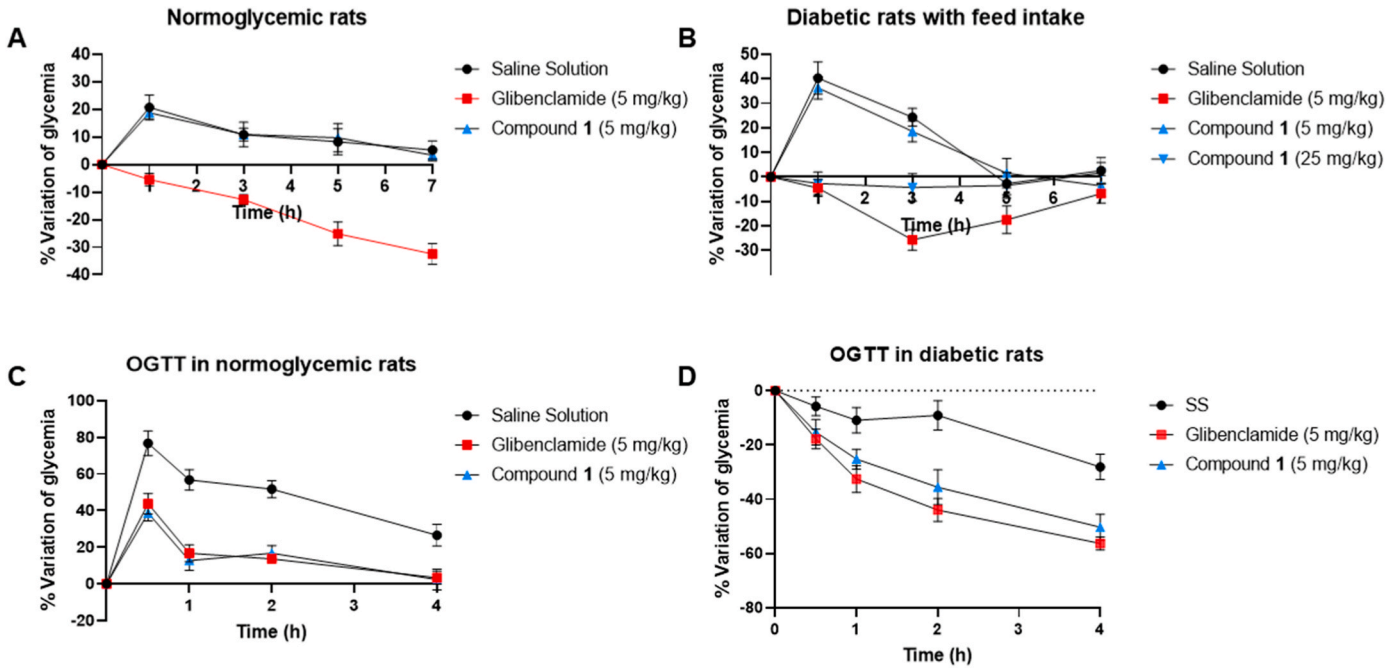


**Fig. 3.** The effect in percent of the variation of glucose for compound 1 in A) Normoglycemic rats, B) Diabetic rats with free feed access; C) and D) Oral glucose Tolerance Test (OGTT) in normoglycemic and diabetic rats, respectively.

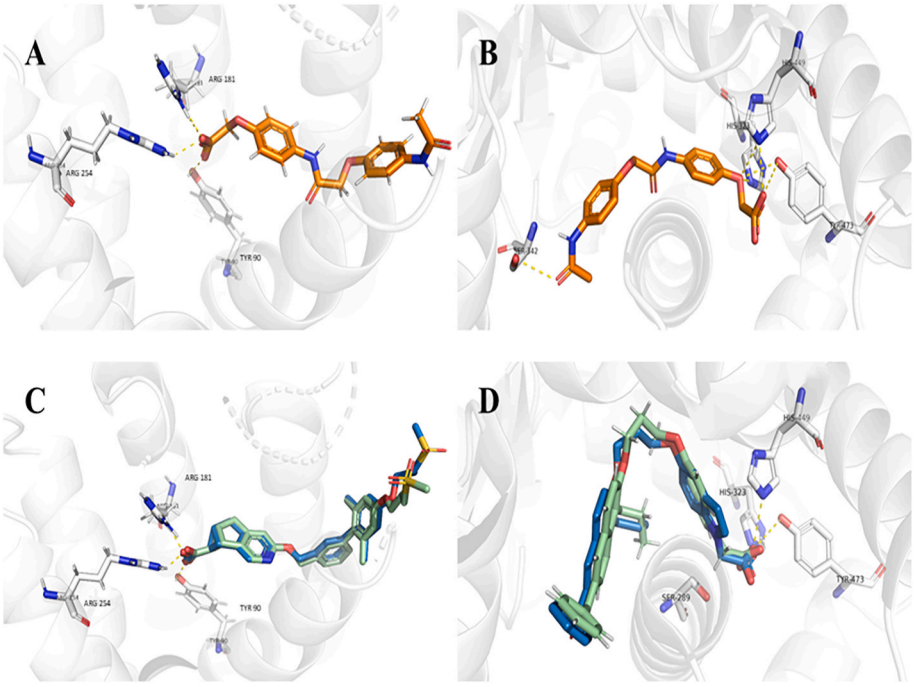


**Fig. 4.** Docked pose (carbon atoms colored orange) of compound 1 and hydrogen bond network is denoted as yellow dashed lines. A) the proposed binding mode of compound 1 with the best free binding energy (−8.4 kcal/mol) in the binding site of GPR40; B) the proposed binding mode of compound 1 with the best free binding energy (−8.2 kcal/mol) in the binding site of PPARγ: C) and D) re-docking pose of co-crystal ligand (carbon atoms colored pale green) with the pose of co-crystal structure reference (carbon atoms colored blue).

varies less, even lower than protein without ligands. The data indicated that the interaction between compound 1 and GPR40 is possibly a partial activation. Fig. 5D showed that the interactions were maintained by a co-crystallized ligand along with the simulation with three main residues. Finally, Fig. 5E illustrates the constituted system used for this simulation.

Also, the behavior of compound 1 was compared and contrasted to the PPARy receptor showing that the co-crystallized ligand maintains polar interactions with the mean residues: His323, His449 and Tyr473 during all simulation (Fig. 6A). Certainly, during the entire process all of the hydrogen bond ranged between 2 and 3 (Fig. 6B) impacting on the stability of the complex; the RMSD obtained during MD (Fig. 6C), which was less than 1.5 Å during and after 20 ns of simulation to compound 1, even lower than the co-crystallized ligand. It is worth mentioning that the co-crystallized ligand undergoes more changes or disturbances than compound 1 in the first 7 ns of simulation, this indicates that the complex of our compound is more stable than the co-crystallized ligand. Besides, Fig. 6D illustrated the interactions between the co-crystallized ligand and receptor that had the mean residues His449 and Tyr473, which were conserved during MD with system were exposed in Fig. 6E.

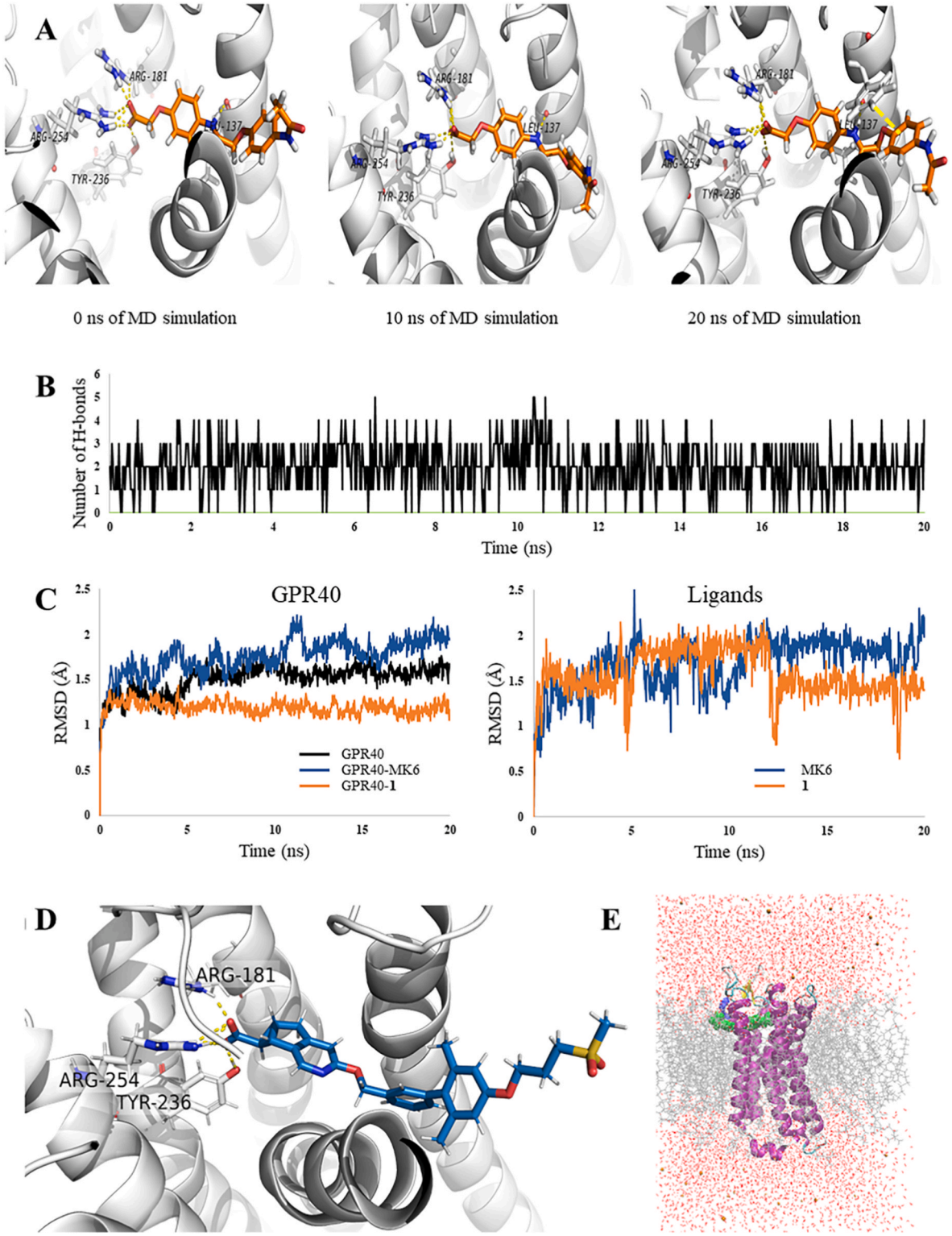


**Fig. 5.** Compound 1 into the binding site of GPR40; A) hydrogen bond network during 20 ns of simulation, B) number of H-bonds during all simulation, C) RMSD of Protein and Ligands, D) final pose of MK6 obtained after of simulation (co-crystal ligand), E) system used for dynamic simulation.

## 4. Discussion

In this work, the final molecules were analogs sharing important characteristics, but the last fragment had some differences, for example, in the case of compound 1 the ending hydrophobic group was acetaminophen while in compound 2 this portion was replaced by 4-hydroxyacetophenone, which had no amidic group. We reported in previous work (Hidalgo-Figueroa et al., 2017) the modification in the same portion, which contained the 2-mercaptobenzimidazole moiety (pre-incubated at 100 μM) demonstrating an increase PPARγ, GPR40 and GLUT4 expression, moreover, showing an increase of $[Ca^{2+}]_i$ levels allowing an increment on insulin release, being as active as the positive control (glibenclamide). However, we have found in the most recent work that this small modification in the molecule allows us to know and

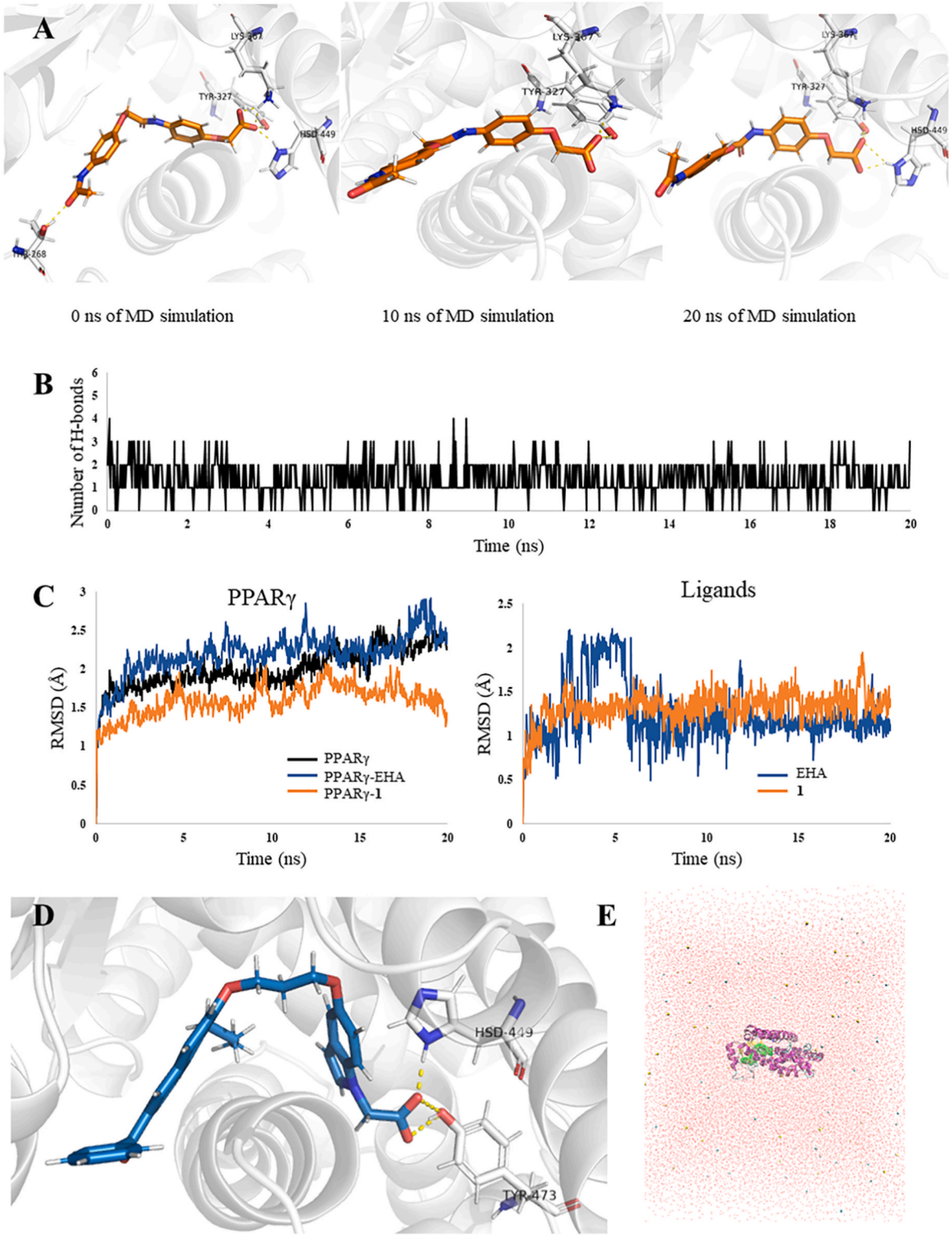


**Fig. 6.** Compound 1 into the binding site of PPARγ; A) hydrogen bond network during 20 ns of simulation, B) number of H-bonds during all simulation, C) RMSD of Protein and Ligands, D) final pose of ligand EHA obtained after of simulation (co-crystal ligand), E) system used for dynamic simulation.

compare the characteristics that increase the potency and details of the molecular requirements to improve the pharmacological activity. Also, this has helped us to be able to discover more effective compounds. Being able to observe that the newly synthesized compound in this work (1, containing acetaminophen structure) has greater potency than the previous molecule since at a lower concentration a similar pharmacological efficacy has been observed. Indeed, it is an important site to consider in the future to modify or preserve in the following design of derivatives.

The increment of PPARγ expression of compound 1 had an impact on GLUT4 expression levels, which are a very important target expressed PPARγ activation. The Increment of GLUT4 expression is associated with glucose uptake and insulin sensibility. Regarding the GPR40 receptor, compound 1 shows a greater effect than the other compounds (2–4),

including higher than glibenclamide (Fig. 2C), which is a novel mechanism reported in a previous publication by our scientific group (Hidalgo-Figueroa et al., 2017).

Correspondingly, we discovered that this release was due to an increase of calcium that affected the mobilization of the vacuoles that contained insulin, which was mild compared to glibenclamide (Fig. 2D and F). For this reason, it can be inferred that compound 1 directly activated the PPARγ receptor and GPR40 receptor.

Also, the observed dose-dependent effect (in vivo) suggests that the dose of 25 mg/kg could be adequate for glycemic control in diabetics and without any adverse effects such as hypoglycemia, which are generated by other drugs such as glibenclamide.

Reviewing the literature, we discovered that the PPARγ full agonists showed undesired side effects associated to these characteristics, which include weight gain, edema, congestive heart failure, and bone fracture. Interestingly, we can observe in the molecular study that compound 1 preserved an interaction with Ser342, which is characteristic of partial agonists (Capelli et al., 2016; Colín-Lozano et al., 2018; Guasch et al., 2011). As compared to the crystallographic ligands, compound 1 preserved numerous important hydrogen bonds with main residues into both targets. Interestingly, three H-bonds were conserved through carboxylic acid in both receptors and these results could explain the experimental findings.

Finally, the ligand reached an equilibrium state characterized by an RSMD profile about 1.5 Å of each complex and relative stable after 15 ns, indicating that the molecular systems remarkably behaved well. The molecular structure of compound 1 had a similar size of co-crystallized ligands in both targets, however, 1 had not an extra tail as MK6 (ligand co-crystallized into GPR40). In contrast, 1 had an extra amidic group in tail compared with EHA (ligand of PPARγ), which indicated that this small hydrogen binding group, as well as the aromatic ring, made the molecules more stable in both receptors and prevented drastic variations in the mode of attachment of compound 1.

## 5. Conclusions

The results suggested that the molecule that had the acetaminophen moiety (compound 1) induced the best control of glucose through the activation of two important and synergic pathways to improve the glucose levels (decreasing of insulin resistance and insulin secretion). Interestingly, compound 1 was pre-incubated at a concentration 9 times lower than the reference drug (pioglitazone) and showed greater activity, which means that it was more potential. Also, it showed an in vivo antidiabetic activity without the hypoglycemic effects from common insulin secretagogues (glibenclamide). The correlation between the in vitro and vivo assay showed the behavior of the compound in an in-silico prediction.

Furthermore, the introduction of a privileged heterocyclic scaffold, as acetaminophen, provides good drug-like properties which in turn lead to more drug-like compounds that have an easy modification to obtain new ligands with requirements in better interaction and safe drugs. In addition, the molecular docking and molecular dynamics simulation revealed the importance on anchoring residues with a pharmacological response. Most importantly, these considerations could be taken into account to design new compounds, which provide promising molecules to improve the treatment of type 2 diabetes.

Finally, it can also be started that the balance in the biological activity that was shown by compound 1 has given a dual property for diabetes treatment on two important targets of glucose control.

## CRediT authorship contribution statement

**Sergio Hidalgo-Figueroa:** Writing – review & editing. **Ana Rodríguez-Luévano:** Writing, Investigation. **Julio C. Almanza-Pérez:** Reviewing, in vitro methodology and Editing. **Abraham Giacoman-Martínez:** in vitro methodology. **Rolffy Ortiz-Andrade:** in vivo methodology, reviewing and editing. **Ismael León-Rivera:** chemical characterization and reviewing. **Gabriel Navarrete-Vázquez:** software and reviewing.

## Declaration of competing interest

The authors declare that there is no conflict of interest regarding the publication of this paper.

## Acknowledgements and Funding

This work was supported by the Consejo Nacional de Ciencia y Tecnología under Grant No. 2001 (APN-2016) and partially supported by FORDECYT No. 296354 and FORDECYT-PRONACES No. 377882. Ana Teresa Rodríguez Luévano acknowledges a Postgrade Scholarship from CONACYT (No. 636061). The authors acknowledge LANEM (CIQ, UAEM) for access to analytical equipment, and Lucia Aldana Navarro for the grammatical review.

## References

Baynest, H.W., 2015. Classification, pathophysiology, diagnosis and management of Diabetes Mellitus. J. Diabetes Metabol. 6 https://doi.org/10.4172/2155-6156.1000541.

Calzada, F., Solares-Pascasio, J., Ordoñez-Razo, R.M., Velazquez, C., Barbosa, E., García-Hernández, N., Mendez-Luna, D., Correa-Basurto, J., 2017. Antihyperglycemic activity of the leaves from Annona cherimolamiller and rutin on alloxan-induced diabetic rats. Pharmacogn. Res. 9, 1–6. https://doi.org/10.4103/0974-8490.199781.

Capelli, D., Cerchia, C., Montanari, R., Loiodice, F., Tortorella, P., Laghezza, A., Cervoni, L., Pochetti, G., Lavecchia, A., 2016. Structural basis for PPAR partial or full activation revealed by a novel ligand binding mode. Sci. Rep. 6 https://doi.org/10.1038/srep34792.

Colín-Lozano, B., Estrada-Soto, S., Chávez-Silva, F., Gutiérrez-Hernández, A., Cerón-Romero, L., Giacoman-Martínez, A., Almanza-Pérez, J., Hernández-Núñez, E., Wang, Z., Xie, X., Cappiello, M., Balestri, F., Mura, U., Navarrete-Vazquez, G., 2018. Design, synthesis and in combo antidiabetic bioevaluation of multitarget phenylpropanoic acids. Molecules 23, 340. https://doi.org/10.3390/molecules23020340.

Darwish, K.M., Salama, I., Mostafa, S., Gomaa, M.S., Khafagy, E.-S., Helal, M.A., 2018. Synthesis, biological evaluation, and molecular docking investigation of benzhydrol- and indole-based dual PPAR-γ/FFAR1 agonists. Bioorg. Med. Chem. Lett 28, 1595–1602. https://doi.org/10.1016/j.bmcl.2018.03.051.

Dodda, L.S., Vilseck, J.Z., Tirado-Rives, J., Jorgensen, W.L., 2017b. 1.14*CM1A-LBCC: localized bond-charge corrected CM1A charges for condensed-phase simulations. J. Phys. Chem. B 121, 3864–3870. https://doi.org/10.1021/acs.jpcb.7b00272.

Dodda, L.S., Cabeza de Vaca, I., Tirado-Rives, J., Jorgensen, W.L., 2017a. LigParGen web server: an automatic OPLS-AA parameter generator for organic ligands. Nucleic Acids Res. 45, W331–W336. https://doi.org/10.1093/nar/gkx312.

Gao, Q., Hanh, J., Váradi, L., Cairns, R., Sjöström, H., Liao, V.W.Y., Wood, P., Balaban, S., Ong, J.A., Lin, H.-Y.J., Lai, F., Hoy, A.J., Grewal, T., Groundwater, P.W., Hibbs, D.E., 2015. Identification of dual PPARα/γ agonists and their effects on lipid metabolism. Bioorg. Med. Chem. 23, 7676–7684. https://doi.org/10.1016/j.bmc.2015.11.013.

Garcia-Macedo, R., Sanchez-Muñoz, F., Almanza-Perez, J.C., Duran-Reyes, G., Alarcon-Aguilar, F., Cruz, M., 2008. Glycine increases mRNA adiponectin and diminishes pro-inflammatory adipokines expression in 3T3-L1 cells. Eur. J. Pharmacol. 587, 317–321. https://doi.org/10.1016/j.ejphar.2008.03.051.

Guasch, L., Sala, E., Valls, C., Blay, M., Mulero, M., Arola, L., Pujadas, G., Garcia-Vallvé, S., 2011. Structural insights for the design of new PPARgamma partial agonists with high binding affinity and low transactivation activity. J. Comput. Aided Mol. Des. 25, 717–728. https://doi.org/10.1007/s10822-011-9446-9.

Hidalgo-Figueroa, S., Navarrete-Vázquez, G., Estrada-Soto, S., Giles-Rivas, D., Alarcón-Aguilar, F.J., León-Rivera, I., Giacoman-Martínez, A., Miranda Pérez, E., Almanza-Pérez, J.C., 2017. Discovery of new dual PPARγ-GPR40 agonists with robust antidiabetic activity: design, synthesis and in combo drug evaluation. Biomed. Pharmacother. 90, 53–61. https://doi.org/10.1016/j.biopha.2017.03.033.

Humphrey, W., Dalke, A., Schulten, K., 1996. VMD: Visual molecular dynamics. J. Mol. Graph. 14, 33–38. https://doi.org/10.1016/0263-7855(96)00018-5.

International Diabetes Federation, 2019. IDF Diabetes Atlas, ninth ed. 7.13.20. https://www.diabetesatlas.org.

Jhun, B.S., Lee, H., Jin, Z.-G., Yoon, Y., 2013. Glucose stimulation induces dynamic change of mitochondrial morphology to promote insulin secretion in the insulinoma cell line INS-1E. PloS One 8, e60810. https://doi.org/10.1371/journal.pone.0060810.

Jorgensen, W.L., Tirado-Rives, J., 2005. Potential energy functions for atomic-level simulations of water and organic and biomolecular systems. Proc. Natl. Acad. Sci. U. S.A. 102, 6665–6670. https://doi.org/10.1073/pnas.0408037102.

Li, Z., Hu, L., Wang, X., Zhou, Z., Deng, L., Xu, Y., Zhang, L., 2019a. Design, synthesis, and biological evaluation of novel dual FFA1 (GPR40)/PPARδ agonists as potential

anti-diabetic agents. Bioorg. Chem. 92, 103254 https://doi.org/10.1016/j.bioorg.2019.103254.

Li, Z., Ren, Q., Wang, X., Zhou, Z., Hu, L., Deng, L., Guan, L., Qiu, Q., 2019b. Discovery of HWL-088: a highly potent FFA1/GPR40 agonist bearing a phenoxyacetic acid scaffold. Bioorg. Chem. 92, 103209 https://doi.org/10.1016/j.bioorg.2019.103209.

Liu, J. (Jim), Wang, Y., Ma, Z., Schmitt, M., Zhu, L., Brown, S.P., Dransfield, P.J., Sun, Y., Sharma, R., Guo, Q., Zhuang, R., Zhang, J., Luo, J., Tonn, G.R., Wong, S., Swaminath, G., Medina, J.C., Lin, D.C.-H., Houze, J.B., 2014. Optimization of GPR40 agonists for type 2 diabetes. ACS Med. Chem. Lett. 5, 517–521. https://doi.org/10.1021/ml400501x.

Loveland, B.E., Johns, T.G., Mackay, I.R., Vaillant, F., Wang, Z.X., Hertzog, P.J., 1992. Validation of the MTT dye assay for enumeration of cells in proliferative and antiproliferative assays. Biochem. Int. 27, 501–510. PMID: 1417886.

Ortiz-Andrade, R., Cabañas-Wuan, A., Arana-Argáez, V.E., Alonso-Castro, A.J., Zapata-Bustos, R., Salazar-Olivo, L.A., Domínguez, F., Chávez, M., Carranza-Álvarez, C., García-Carrancá, A., 2012. Antidiabetic effects of Justicia spicigera Schltdl (Acanthaceae). J. Ethnopharmacol. 143, 455–462. https://doi.org/10.1016/j.jep.2012.06.043.

Papaetis, G.S., Papakyriakou, P., Panagiotou, T.N., 2015. State of the art paper Central obesity, type 2 diabetes and insulin: exploring a pathway full of thorns. Arch. Med. Sci. 11, 463–482. https://doi.org/10.5114/aoms.2015.52350.

Parimala, M., Debjani, M., Vasanthi, H.R., Shoba, F.G., 2015. Nymphaea nouchali Burm. f. hydroalcoholic seed extract increases glucose consumption in 3T3-L1 adipocytes through activation of peroxisome proliferator-activated receptor gamma and insulin sensitization. "J. Adv. Pharm. Technol. Research"" (JAPTR)" 6, 183–189. https://doi.org/10.4103/2231-4040.165013.

Pettersen, E.F., Goddard, T.D., Huang, C.C., Couch, G.S., Greenblatt, D.M., Meng, E.C., Ferrin, T.E., 2004. UCSF Chimera-A visualization system for exploratory research and analysis. J. Comput. Chem. 25, 1605–1612. https://doi.org/10.1002/jcc.20084.

Phillips, J.C., Braun, R., Wang, W., Gumbart, J., Tajkhorshid, E., Villa, E., Chipot, C., Skeel, R.D., Kalé, L., Schulten, K., 2005. Scalable molecular dynamics with NAMD. J. Comput. Chem. 26, 1781–1802. https://doi.org/10.1002/jcc.20289.

Ribeiro, J.V., Bernardi, R.C., Rudack, T., Stone, J.E., Phillips, J.C., Freddolino, P.L., Schulten, K., 2016. QwikMD — Integrative molecular dynamics toolkit for novices and experts. Sci. Rep. 6 https://doi.org/10.1038/srep26536.

Rodrigues, D.A., Pinheiro, P.S.M., Ferreira, T.T.D.S.C., Thota, S., Fraga, C.A.M., 2017. Structural basis for the agonist action at free fatty acid receptor 1 (FFA1R or GPR40). Chem. Biol. Drug Des. 91, 668–680. https://doi.org/10.1111/cbdd.13131.

Shapovalov, M.V., Dunbrack, R.L., 2011. A smoothed backbone-dependent rotamer library for proteins derived from adaptive kernel density estimates and regressions. Structure 19, 844–858. https://doi.org/10.1016/j.str.2011.03.019.

Sum, C.S., Tikhonova, I.G., Neumann, S., Engel, S., Raaka, B.M., Costanzi, S., Gershengorn, M.C., 2007. Identification of residues important for agonist recognition and activation in GPR40. J. Biol. Chem. 282, 29248–29255. https://doi.org/10.1074/jbc.m705077200.

Vieira, R., Souto, S.B., Sánchez-López, E., Machado, A.L., Severino, P., Jose, S., Santini, A., Fortuna, A., García, M.L., Silva, A.M., Souto, E.B., 2019. Sugar-lowering drugs for type 2 diabetes mellitus and metabolic syndrome—review of classical and new compounds: Part-I. Pharmaceuticals 12, 152. https://doi.org/10.3390/ph12040152.

Wu, B., Wei, S., Petersen, N., Ali, Y., Wang, X., Bacaj, T., Rorsman, P., Hong, W., Südhof, T.C., Han, W., 2015. Synaptotagmin-7 phosphorylation mediates GLP-1–dependent potentiation of insulin secretion from β-cells. Proc. Natl. Acad. Sci. U.S.A. 112, 9996–10001. https://doi.org/10.1073/pnas.1513004112.